Nuclear Engineering and Technology 51 (2019) 284–292

Contents lists available at ScienceDirect

Nuclear Engineering and Technology

journal homepage: www.elsevier.com/locate/net

Original Article

On the Particle Swarm Optimization of cask shielding design for a prototype Sodium-cooled Fast Reactor

Dong-Won Lim [a], Cheol-Woo Lee [b], Jae-Yong Lim [c], Donny Hartanto [d, *]

[a] Department of Mechanical Engineering, University of Suwon, 17 Wauan-gil, Bongdam-eup, Hwaseong-si, Gyeonggi-go, 18323, Republic of Korea
[b] Nuclear Data Center, Korea Atomic Energy Research Institute (KAERI), Daedeok-daero 989-111, Yuseong-gu, Daejeon, 34057, Republic of Korea
[c] SFR Reactor Design Division, Korea Atomic Energy Research Institute (KAERI), Daedeok-daero 989-111, Yuseong-gu, Daejeon, 34057, Republic of Korea
[d] Department of Mechanical and Nuclear Engineering, University of Sharjah, P.O. BOX 27272, Sharjah, United Arab Emirates

ARTICLE INFO

Article history:
Received 25 June 2018
Received in revised form
27 August 2018
Accepted 14 September 2018
Available online 17 September 2018

Keywords:
Fuel transfer cask
Radiation shielding
MCNP
Particle Swarm Optimization (PSO)
Sodium-cooled Fast Reactor Refueling

ABSTRACT

For the continuous operation of a nuclear reactor, burnt fuel needs to be replaced with fresh fuel, where appropriate (ex-vessel) fuel handling is required. Particularly for the Sodium-cooled Fast Reactor (SFR) refueling, its process has unique challenges due to liquid sodium coolant. The ex-vessel spent fuel transportation should concern several design features such as the radiation shielding, decay-heat removal, and inert space separated from air. This paper proposes a new design optimization methodology of cask shielding to transport the spent fuel assembly in a prototype SFR for the first time. The Particle Swarm Optimization (PSO) algorithm had been applied to design trade-offs between shielding and cask weight. The cask is designed as a double-cylinder structure to block an inert sodium region from the air-cooling space. The PSO process yielded the optimum shielding thickness of 26 cm, considering the weight as well. To confirm the shielding performance, the radiation dose of spent fuel removed at its peak burnup and after 1-year cooling was calculated. Two different fuel positions located during transportation were also investigated to consider a functional disorder in a cask drive system. This study concludes the current cask design in normal operations is satisfactory in accordance with regulatory rules.

1. Introduction

A Sodium-cooled Fast Reactor (SFR) is one of Generation IV (Gen-IV) reactors and is in the development step for up to the commercialization level. SFR is a nuclear reactor using fast neutrons. The coolant is liquid sodium in that it has an excellent performance in conductivity. Also, it melts at 371 K and boils at 1156 K, and so SFR does not need to be pressurized in general. The design goals of Gen-IV SFRs include improved safety, sustainability, efficiency, cost, and proliferation resistance [1,2]. One of the key elements to fulfill SFR goals is a fuel handling system (FHS), which transfers highly radioactive materials. FHS requires its stringent level of safety and integrity against functional disorder or boundary breakage from the outside (both for physical leakage and for radiological shielding). Moreover, an efficient but reliable fuel handling method can make not only constructional but also operational costs low. The FHS design task sees challenges in order to satisfy all the design criteria due to a number of constraints such as opacity of sodium coolant, a unique working environment in sodium and inert gas environment, a moving path across the pressure boundary, radiation risk, tight construction layout, and so forth. Sodium rapidly reacts with air and water producing heat and fire. In other words, SFRs need to maintain the pressure boundary between air and inert regions all the time even during the refueling period. For this reason, refueling in modern SFRs is performed with the reactor vessel head (or cover) closed.

A cask, which is a shipping container to transfer nuclear (or radioactive) materials, is one of FHS components. Typically, a cask is used to transport spent nuclear fuel from nuclear power plants to disposal sites (or reprocessing facilities). A cask is designed for its functional purposes. For example, an inter-building cask (IBC) is to be used between a reactor and fuel buildings in the same plant site, or other types can be for transportation of nuclear waste from the plant to remote disposal sites. Particularly, IBC is interesting in the design perspective, because its design to deal with very high radioactive material just out of the core at high temperature is

* Corresponding author.
E-mail address: dhartanto@sharjah.ac.ae (D. Hartanto).

https://doi.org/10.1016/j.net.2018.09.007

challenging. In general, shielding radioactive by-products to reduce radiations blocks the heat exchange pathways, and thus one counteracts the other between shielding and cooling off the by-products. Furthermore, the IBC of SFRs is located at the pressure boundary, and this means the design demands an additional requirement for leak tightness.

A spent fuel is the highest radioactive material among nuclear by-products. It is required to be replaced with a fresh one from a fuel building where new and spent fuels are processed and stored. When refueling, spent fuel assemblies (FAs) are unloaded from the core by a gripper of the in-vessel handling machine (IVHM) with or without rotating plug(s) in the vessel head, transferred out of the reactor vessel (RV), stored in a cask (or shoot) moved by an ex-vessel transportation machine (EVTM), and shipped to sodium treating stations. For some reactors employed an ex-vessel storage (EVS) where a spent FA brought out of a reactor is stored for extra cooling. Also, an in-vessel storage (IVS) is used for cooling spent FAs in the vessel. The utilization choice of IVS and EVS mainly depends on the SFR size in thermal-/electric-output—the subsequent decay heat of spent FAs—and the number of drive FAs. In the view of the EVS cost, Chikazawa et al. [3] used the primary sodium storage and ex-vessel transfer methods to categorize the refueling system type into four groups: A) neither IVS nor EVS, B) only IVS, C) EVS alone, and D) both IVS and EVS equipped. Even though IBC design depends on the choice of IVS and EVS, it is typical that spent FAs are removed from the core through IVHM and IBC to the fuel building.

Compared with casks for pressurized water reactors, there are just a few SFR cask designs, since the SFR is yet to be commercialized (SFR casks are relatively new and still under development). Nevertheless, a few cask design practices were reported in the literature. Among some notable types, a cask called an inter-building coffin (as an IBC) was developed for Experimental Breeder Reactor II (EBR-II), which was a 62.5 MWth sodium-cooled fast reactor that produced an electrical output of 20 MW. The IBC carried the spent fuel to the fuel cycle facility, and its cooling capacity with inert gas was 1.2 kW [4,5]. The Fast Flux Test Facility (FFTF), operated from 1982 to 1992 in Washington US, was a 400 MWth sodium-cooled experimental fast reactor. For FFTF, the bottom-loading transfer cask (BLTC) was developed to remove the spent fuel from the core and transfer it to a sodium-filled vessel in the fuel storage facility after 1 year of decay time. The BLTC was cooled with argon and had a maximum cooling capacity of 1.4 kW. The BLTC also transferred fresh fuel from the core component conditioning station [6]. Prototype Fast Breeder Reactor (PFBR) is a 1250 MWth, 500 MWe sodium-cooled, and pool-type reactor in India [7]. In PFBR, all the sub-assemblies pass through the Fuel Transfer Cell. It is a rectangular cell in the fuel handling building with concrete walls lined with stainless steel. This becomes a pathway to the reactor vessel from the inclined fuel transfer mechanism and inclined underwater trolley for fresh and spent subassemblies, respectively [8]. ASTRID (Advanced Sodium Technological Reactor for Industrial Demonstration) from France is a 600 MWe sodium-cooled fast breeder reactor project, proposed by the Commissariat a l'energie atomique (CEA). It plans to be commissioned for the demonstration in the 2020's. ASTRID considers the refueling ramp, transfer lock, and gas corridor [9]. Dechelette et al. [9] compared refueling options, and cask and direct fuel handling were among them. It consists of a cask casing (shield), a sodium pot (where the irradiated assembly is cooled), a fuel grabbing tube, and a cask cooling system. The cooling system architecture is done by argon flowing in a circuit in the cask and cooled down by the units outside the cask by blowers, which have a capacity to cool off a high residual heat around 40 kW. The authors argue that cask and direct fuel handling are expensive and high safety risk. Also, it requires a very long development and qualification time. The Japan Sodium-cooled Fast Reactor (JSFR), which is currently under conceptual study [10], is a 750MWe demonstration reactor (total 1500 MWe at the plant site). The spent fuel storage in the EVS tank during one operation cycle and the reduced decay heat is less than 10 kW to handle in an inert-gas area. EVTM with argon gas cools a sodium pot with a spent fuel in the coffin [11].

PFBR, ASTRID, and JSFR commonly employs (or considers at least) an EVS to store fuel assemblies and to reduce the heat. Despite the high EVS cost, EVS effectively provides a buffer space that allows preheating fresh FAs and cleaning spent FAs while the reactor is operating. Thus, EVS is appropriate for large SFRs such as PFBR, ASTRID, and JSFR with a greater number of FAs to facilitate refueling process. But, this may not be applicable to a prototype reactor (or a modular type reactor) which electric output is at most ~150 MWe (smaller than commercial size reactors), and it may consider only an IVS instead of an EVS. A ramp refueling option with a large inert cell was adopted in commercial grade plants such as PFBR and ASTRID, but the option may not be affordable for a prototype (small) reactor, either. (For PFBR, it is referred as Inclined Fuel Transfer Mechanism.) Thus, for a prototype size, a dry-type ex-vessel refueling without a sodium pot is generally selected. And the IBC design becomes challenging to deal with the trade-off relationship between shielding and cooling.

In this design study, an optimization design approach of the spent fuel cask has been proposed for a prototype-size SFR. The chosen reactor is a generic pool-type SFR with two intermediate heat transport system loops with two steam generators as appeared in Prototype Gen-IV Sodium-cooled Fast Reactor [12]. Its thermal and electric output is ~400 MWth and ~150 MWe, respectively, with about 100 U-10Zr driver FAs at its initial fuel loading and U-TRU-Zr later. The overall refueling method is to be customized to the reactor (or fuel) specifications: the radioactivity level, thermal size, and fission material. The refueling system of the study is illustrated in Fig. 1. In the perimeter of the core region, IVS is located to cool off spent FAs for approximately 10 months prior to transportation. A fixed arm charge machine (FACM) as IVHM, being accessible to whole core FAs in combination of rotating small and

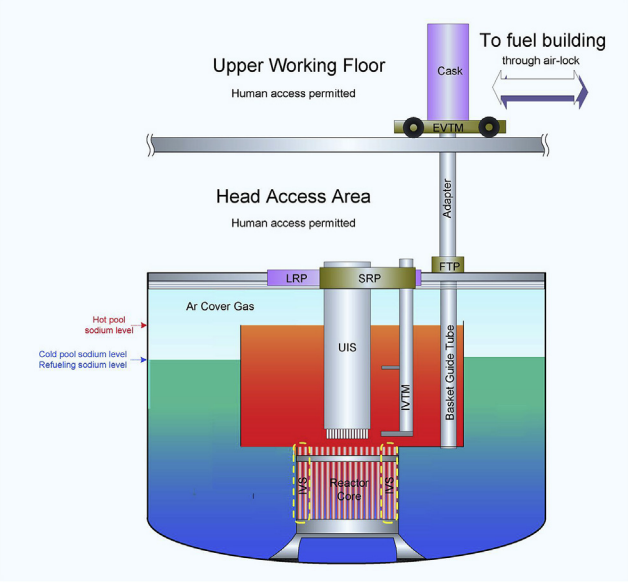

Fig. 1. Overall concept of refueling system.

large rotatable plugs (SRP and LRP, respectively), picks up an FA one by one. A spent FA gripped by FACM is moved to the cask located in the upper working floor through the gate valve of the fuel transfer port (FTP) in the reactor head guided by the basket guide tube. Self-motorized EVTM, the cask carriage, provides an inert environment of the FA pathway, and goes back and forth between the reactor and fuel buildings passing an air-lock gate.

The shielding thickness of the spent fuel cask t_s is the primary design variable in the design optimization. It is easily expected that t_s has an inversely proportional relation with the shielded dose rate. Even though the passing air through the inner cooling duct can carry the heat to the outside, a thick t_s has an adverse effect on cooling. Also, a thick t_s will make the cask heavy, and a heavy cask is neither economic nor easy to operate in a plant building. Thus, the Particle Swarm Optimization (PSO)—an optimization technique to choose an appropriate t_s value in considerations of the shielding performance and its weight—was taken for an efficient design approach.

PSO [13,14] is an optimization algorithm developed based on the social behavior reflected in the flock of birds, bees, and fish that adjust their movements to seek foods or to avoid predators. PSO is known as a robust and viable method to handle non-linear, non-convex design spaces with discontinuities [15]. But also, it can handle continuous, discrete and integer variable types with ease. Furthermore, PSO is more efficient, requiring only a few numbers of function evaluations for better results (or at least the same quality of results) [16,17].

In this work, MCNP6 (Monte Carlo N-Particle version 6) code [18] in conjunction with ENDF/B-VII.0 nuclear data library has been used to perform the radiation shielding calculation of the SFR spent fuel cask. MCNP is a general and powerful code to analyze the neutrons, photons, and electrons transport including their radiation dose. It has been widely used for example to calculate the dose of light water reactor spent fuel storage cask [19,20]. Compared with the deterministic radiation shielding codes, MCNP has several advantages such as it can model a complicated three-dimensional geometry and it uses the continuous energy cross-section of the particle. To improve the speed of the calculation and the accuracy, the weight window variance reduction technique has been employed in the calculation.

The overall cask design concept of study is briefly presented in Section 2, followed by the target reactor's source term calculation. Optimization of the conflict design variables for the given model is discussed in Section 4. And, the MCNP analysis and the results are given afterwards. The last section summarizes this study and gives concluding remarks together with future work.

2. Cask design concept

The fuel transfer cask design must satisfy design requirements, which are described to ensure safety and to protect persons, property and the environment from the effects of radiation in the transport of radioactive material. The standards specify following requirements: 1) the radioactive contents should be contained in matters such as packages and conveyance; 2) external radiation levels should be controlled; 3) criticality should be prevented; and 4) damage caused by heat should be prevented [21]. Particularly, for SFR spent fuel assemblies, liquid sodium-wetted assembly body should be in an inert environment blocked from water or air, because sodium can violently react with water and air, causing fire or fumes.

Fig. 2 illustrates the cask design concept in a cutaway view. The cask contains one fuel assembly each time of the refueling process. The cask is a double-cylinder structure for shielding and cooling. The outer cylinder, made of mainly lead, shields radiations, and the inner cylinder, separates the inert space from the cool air passing through a swirling airway between cylinders. In the inner cylinder, made of stainless steel, the basket with or without a fuel assembly moves up and down. The inner cylinder is sealed, completely blocked from the air, and securely fixed in the outer cylinder. The inner cylinder is actively cooled by the atmospheric air to remove the decay heat of the spent fuel. The decay heat is primarily cooled by inert gas in the inner cylinder. The cooling air in between reduces the temperature difference of the in-and-out lead shields and the consequent structural expansion. This double-cylinder design feature makes it available to separate the design considerations for shielding and cooling.

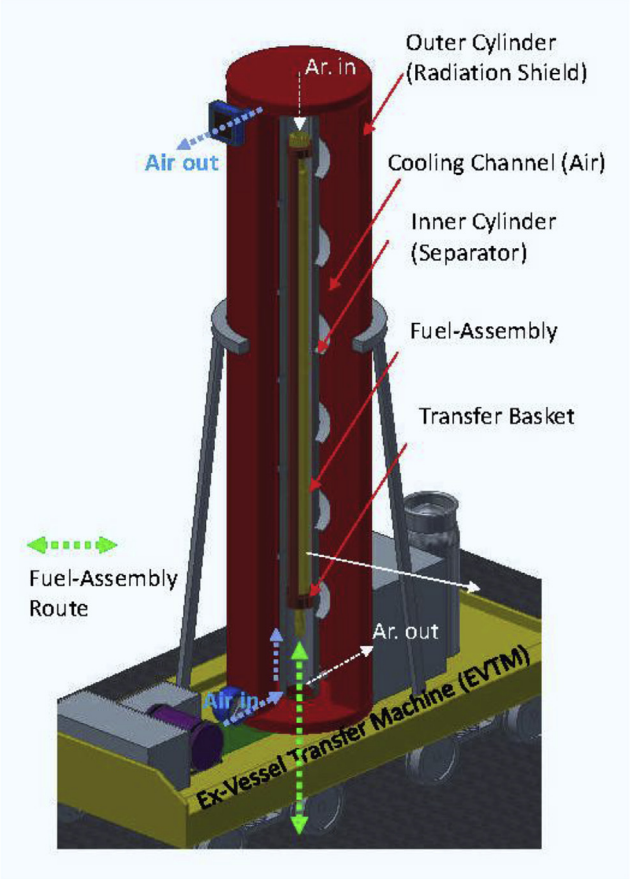

Fig. 2. Cask design concept as a double-cylinder structure.

In the figure of the cask design concept, the right inset displays the gate valve mechanism in the bottom of the cask. Once the bellows is connected to the adapter and tightly sealed, the sliding gate valve is opened. Then, the fuel transfer basket can freely move to and from the reactor vessel vertically.

The connecting cable, when the cable is used for a motion medium, is dipped in the sodium when lowering the basket in the vessel. To retain the dipped portion in the inert space, the cable is turned around from the top of the cask down to the bottom. The cask is connected to the winch chamber, where the basket driving winch is located. The winch cell is also contained and maintained in an argon atmosphere. The argon is circulated for purging from the top to bottom in the inner cylinder.

The primary design parameters are the shielding thickness of the outer cylinder t_s, the cooling gap width between cylinders t_c, and the inner cylinder diameter as shown in Fig. 4. The inner cylinder diameter t_i is predetermined as 300 mm by associated components' designs of the fuel assembly and moving basket.

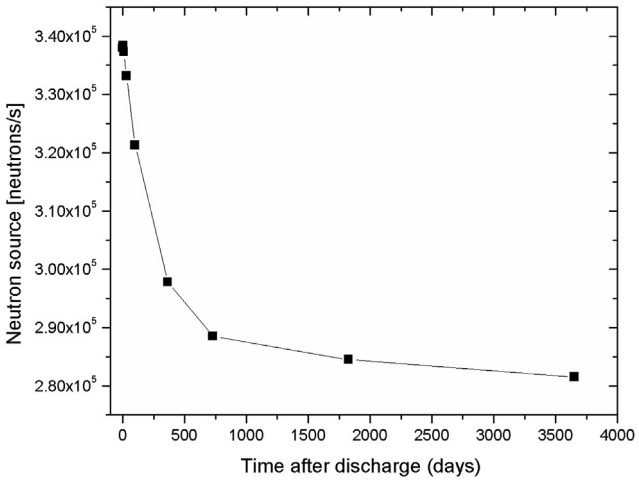

Fig. 3. Spontaneous neutron source of discharged fuel.

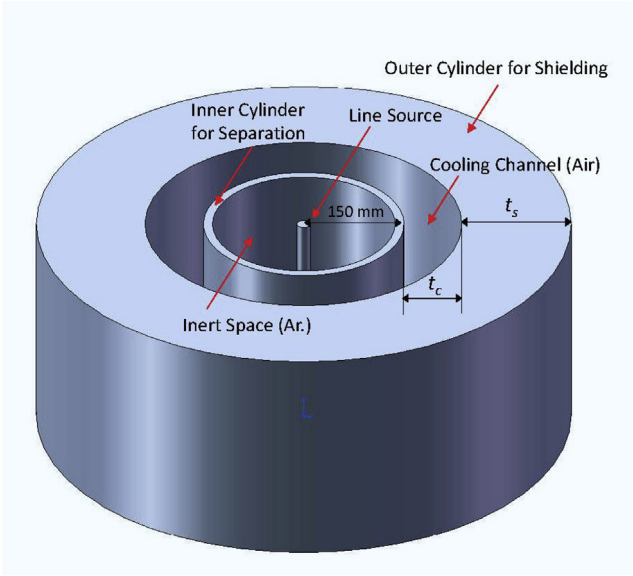

Fig. 4. Simplified cask model for an optimization algorithm.

3. Source term calculation

The radiation source term of the spent fuel is necessary for the multi-group shielding analysis. For the first batch cycle of SFR, fresh fuel at U-10Zr is loaded. It is assumed that the fuel was irradiated up to a specific burnup of 107 GWd/t for 4–5 cycle terms, about 3–4 years. Photons in the spent nuclear fuel are the major radioactive sources during fuel transportation from the IVS to the fuel storage facility. Decay gammas of fission products, activation products, and actinides are major gamma sources, but there are prompt gammas that are generated by spontaneous fissions of actinides. For conservative evaluation, the gammas of the used fuels having peak burnup are provided in Table 1 [12] at the charge, discharge, discharge after various periods of cooling at IVS for 365, 395, and 425 days, calculated using ORIGEN2 [22]. Discharging a peak burnup fuel assembly means removing a driver fuel at the specific burnup of 107 GWd/t mentioned earlier.

As displayed in Table 1, the radiation stream rate is the strongest at 0.02 MeV among other energy groups, when the fuel is taken out at its peak burnup. And the rate exponentially decreases over the cooling time. However, the decay rate is only about 12% smaller comparing the rates between 1-year cooling and 395-day cooling. Therefore, after 1-year cooling, spending more time for cooling is not greatly effective.

Fig. 3 shows the neutron source rate of the most reactive fuel after discharged. The rate of the spontaneous neutron source from the decay of the fission products and heavy metal is much lower than the gamma source rate by a factor of 10^{11}. Due to this reason, the impact of the neutron source is not considered in this study.

4. Initial design value setting by Particle Swarm Optimization

The optimization process requires design iterations. At each iteration, the radiation dose rate and cask weight are calculated every time. If a full 3-dimensional model is considered for this process, the calculation load, particularly for the shielding analysis, becomes very heavy, and the process becomes ineffective. And different tally locations in the shielding analysis should be selected for changed geometry after iterations, and this leads to an inconsistent optimization result. Thus, a simplified cask model as shown in Fig. 4 is used for the calculations. The model is elongated from the same cross-sectional shape and is cut into a unit length to assess the radial radiation dose rate at its surface and cask weight.

The particle swarm process is stochastic in nature. The algorithm uses a velocity vector to update the current position of each particle in the swarm. The velocity vector flies through the search space by following the current optimum particle gained from the particle's memory after iterations (cognitive behavior) and the knowledge gained by the whole swarm (social interaction). Thus, the position of each particle in the swarm is updated based on the social behavior of the swarm which adapts to its environment by returning to promising regions of the space previously discovered and searching for better positions over time.

For the cask design problem, the cask shielding thickness t is taken as a variable to minimize the objective function value by PSO. The thickness value t_k^i is called a position of a particle i at iteration k to be updated by Eq. (1).

$$t_{k+1}^i = t_k^i + v_{k+1}^i \Delta s \quad (i = 1, \ldots, n), \tag{1}$$

where v_{k+1}^i is the velocity vector of the particle i at iteration k to be updated by the individual and swarm behavior, Δs is the time step size, and n is the number of particles [21]. By PSOthe velocity v_{k+1}^i is updated by Eq. (2) as

$$v_{k+1}^i = w v_k^i + c_1 r_1 \frac{\left(p_k^i - t_k^i\right)}{\Delta s} + c_2 r_2 \frac{\left(p_k^g - t_k^i\right)}{\Delta s}. \tag{2}$$

In the equation, r_1 and r_2 are random numbers between 0 and 1; p_k^i and p_k^g represent the best particle position in the particle i movements and the global best position in the swarm up to k. The trust parameters are used for weighing on cognitive and social behavior, depending on problems. The weight parameters w indicate the confidence on each behavior of two, as c_1 and c_2 are on the cognitive and social behavior, respectively. These weight parameters are employed to control the exploration abilities of the swarm.

The objective function is dictated by the design goal of shielding radiation as low as achievable with light weight. Obviously, thicker the shielding wall is, lower the dose rate on the cask outer surface can be. However, a thick wall makes the cask heavy, and it may not be able to be operated in the reactor and fuel buildings. Thus, the objective function J is given in the sum of squares by two design measures as

Table 1
Photon source term calculation results [photons/s].

Photon upper bound energy (MeV)	Charged fuel	Discharged fuel	1-year cooling	395-day cooling	425-day cooling
2.0E-02	6.99E+08	4.63E+17	4.43E+15	4.15E+15	3.90E+15
3.0E-02	0.00E+00	9.14E+16	9.79E+14	9.23E+14	8.71E+14
4.5E-02	9.50E+05	7.76E+16	1.01E+15	9.48E+14	8.92E+14
7.0E-02	5.94E+05	8.05E+16	8.58E+14	8.05E+14	7.57E+14
1.0E-01	8.12E+07	1.11E+17	6.16E+14	5.78E+14	5.43E+14
1.5E-01	1.60E+08	1.03E+17	7.41E+14	6.92E+14	6.47E+14
3.0E-01	5.67E+08	1.62E+17	5.23E+14	4.91E+14	4.61E+14
4.5E-01	1.42E+06	8.86E+16	3.08E+14	2.91E+14	2.76E+14
7.0E-01	6.96E+04	1.48E+17	2.03E+15	1.97E+15	1.91E+15
1	1.09E+04	1.61E+17	3.03E+15	2.74E+15	2.49E+15
1.5	6.69E+02	8.71E+16	1.06E+14	1.01E+14	9.67E+13
2	3.27E+02	3.17E+16	1.03E+13	9.62E+12	9.02E+12
2.5	1.90E+02	1.68E+16	2.59E+13	2.41E+13	2.24E+13
3	1.10E+02	7.28E+15	2.82E+11	2.66E+11	2.51E+11
4	9.84E+01	3.85E+15	3.40E+10	3.21E+10	3.04E+10
6	4.23E+01	1.85E+15	1.20E+04	1.18E+04	1.16E+04
8	4.87E+00	1.54E+13	1.34E+03	1.32E+03	1.30E+03
11	5.60E-01	3.89E+09	1.52E+02	1.49E+02	1.47E+02
Total	1.51E+09	1.64E+18	1.47E+16	1.37E+16	1.29E+16

$$J = \gamma^2 + \mu^2, \tag{3}$$

Where γ and μ represent the normalized radiation dose rate and the total weight of the shield, respectively. Each evaluation term was divided by corresponding desirable values (2 mrem/h for the dose rate and 50 tons for the weight were taken for the case study). These values can be adopted from design requirements such as NRC (Nuclear Regulatory Commission) Title 10, Code of Federal Regulations [23]. Note that the calculated thickness value is an initial choice from an optimization process, and the value can be varied by 3-dimensional evaluations.

By utilizing the particle and velocity updates in the mentioned equations, the PSO algorithm is constructed as shown in Fig. 5, which flowchart illustrates the overall PSO procedure. The first step is to initialize a set of n particles of the position t_k^i and velocity v_k^i. The particles are randomly distributed throughout the design space bounded by specific limits. Next, the chosen values are evaluated by the objective function given in Eq. (3). If the stopping criteria of the iteration loop are not met, two consecutive update steps are followed: 1) update the optimum particle p_k^i and global optimum particle position p_k^g; and 2) update the position of the next particle using its previous position and updated velocity vector as described in Eqs. (1) and (2).

The initial particles are selected randomly in the allowable range of (t_{min} , t_{max}) by using Eqs. (4) and (5) as follows:

$$t_0^i = t_{min} + r(t_{max} - t_{min}), \tag{4}$$

$$v_0^i = \frac{t_{min} + r(t_{max} - t_{min})}{\Delta s}. \tag{5}$$

To evaluate the PSO objective function at various thicknesses, corresponding radiation dose rates were calculated by the MCNP6 sensitivity study. The study, using the simplified cask model presented earlier, yielded discrete dose rate data for the objective function to be calculated at each optimization process. Shielding analysis was carried out by MCNP6 code technique [13]. In this study, major shielding sources are on the effects by photons. The sensitivity study on the radiation shielding performance as a function of the shielding thickness is shown in Fig. 6. As shown in this figure, the dose rate decreases over the shielding thicknesses in the range of 25–35 cm, and its rate is faster than the exponential decay function. As displayed, the error bars on the examined

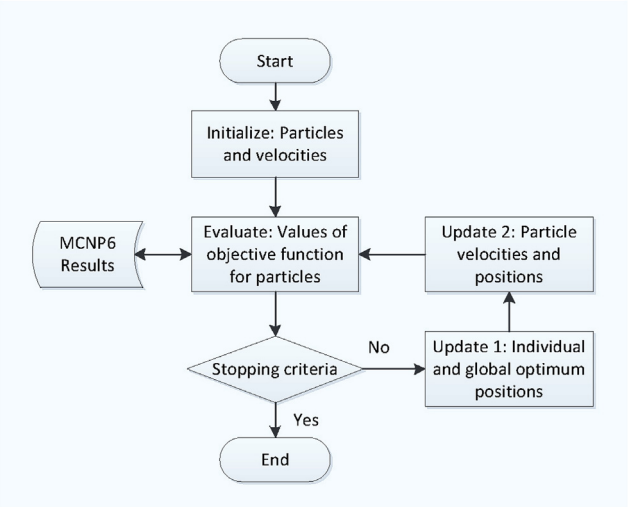

Fig. 5. The searching process of the PSO algorithm.

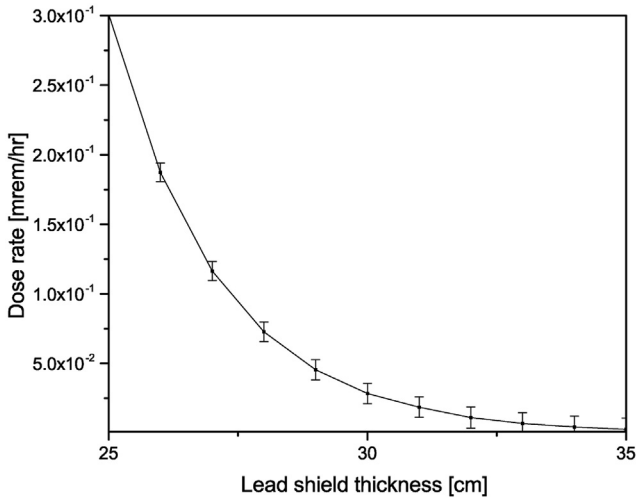

Fig. 6. Radiation dose vs. the shielding thickness.

thickness are relatively small within 1% error. In the plot, a continuous curve was generated by interpolating discrete data points. Also, the interpolation as shown was employed in the optimization process.

5. Shielding analysis

The cask shielding materials and structures are chosen based on the PSO process results to reduce mainly gamma radiation. Shielding analysis was carried out by the same MCNP6 code as done in the earlier section. The same major shielding sources from photons were considered as well. The optimization results of the searching process for the shielding thickness as shown in Fig. 7 converges very quickly in just 5 iterations. And only ten random particles were utilized, converging to the fitness value of 25.7 cm. It is noted that more random PSO particles gave a similar result. With different weight settings, the converged fitness values had small differences to 26 cm. The final value was conservatively chosen as 29 cm with about 10% safety margin.

For the final design evaluation, the radiation levels were analyzed for the 3D cask design. Shields which are made of lead are represented in a red color. Thicknesses are 290 and 100 mm in radial and top/bottom directions as shown in Fig. 8 as given in a side cut-view, simplified geometries in the interests of gamma shielding. The fuel is stored in 395 an inner cylinder of 320 mm diameter colored in green. The area in green is an inert space filled with argon gas. The argon gas is inserted through an inlet to an outlet of 40 mm and 58 mm diameters, respectively. The inert inner cylinder is a containment separated and sealed. The containment is air-cooled, and this air cooling space by a 150 mm gap is in white. For this air cooling, at top and bottom, 100 mm holes in diameter are for the outlet and inlet, respectively. Except for lead shields, most structures are made of austenitic stainless steel. The fuel assembly in this analysis was modeled as components of the top plug,

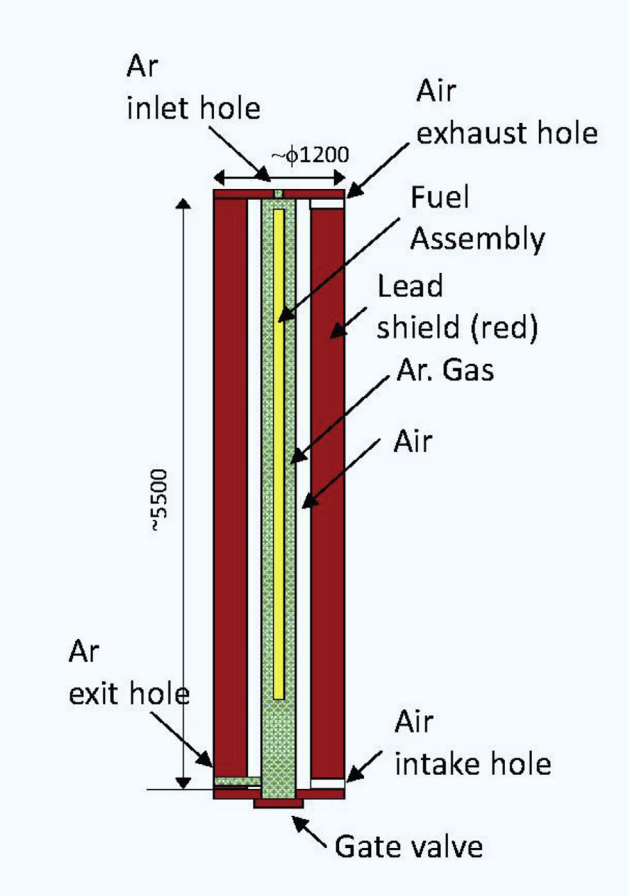

Fig. 8. Simplified geometry for radiation shielding in a side cut-view.

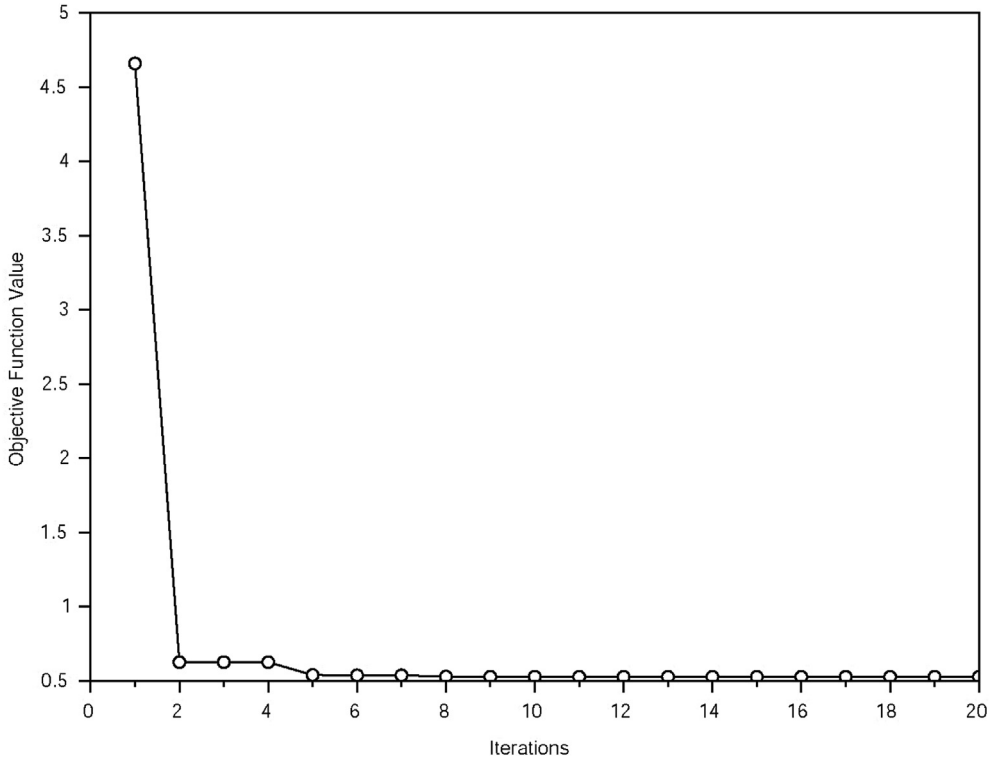

Fig. 7. The searching process for optimum shielding thickness.

top reflector, gas plenum, active fuel region, mounting rail, and lower reflector. For the FA energy spectrum analysis, the active region is set uniform in its axial direction.

The MCNP model is shown in Fig. 9 in its side and top cut-views. The analysis is set as two transportation scenarios: 1) FA stored at the bottom, and 2) FA at the top. The atomic number density for a U-10Zr spent fuel assembly in this study for each isotope is listed in Table 2.

Table 2
Fuel composition at discharge.

Isotope	Atomic density [atom/barn-cm]
U-234	1.39875E-08
U-235	3.05510E-03
U-236	3.11058E-04
U-238	1.88709E-02
Pu-238	1.73640E-06
Np-237	1.70791E-05
Pu-239	7.01279E-04
Pu-240	2.46943E-05
Pu-241	6.51982E-07
Pu-242	1.35156E-08
Am-241	2.62574E-08
Am-242 m	3.29727E-10
Am-243	2.20655E-10
Cm-242	6.14316E-10
Cm-243	4.59310E-12
Cm-244	1.04257E-11
Cm-245	1.96964E-13
Cm-246	2.88179E-15
Zr	7.65323E-03
Fission products	1.39875E-08

6. Shielding analysis result

The shielding analysis had been done by the MCNP6 calculations using the model shown in Fig. 9. The calculations provided are on the evaluations of a gamma radiation dose. Four analysis cases were performed: removing an FA at its peak burnup and after 1 year-long cooling at 420 IVS when carrying an FA at its top and bottom position. The evaluation results were compared with regulatory standards. Tally locations of dose detector points are displayed in Fig. 10. Location (1) is an inert-gas inlet, (2) is an air outlet, (3) is a cask radial surface, (4) is an inert-gas outlet, (5) is an air inlet, and (6) is the gate valve surface. The MCNP6 code technique was applied by using the mesh-based weight window variance reduction function. This method requires triple iterations each time for its convergence with the photon calculation option. As a result, the relative error at the location (3), the cask surface, was from 0.03% to 0.34%. The MCNP6 default flux-to-dose conversion factor ICRP-21 1971 was adopted in this study.

The shielding analysis results on the spent fuel removed at its peak burnup and after 1-year cooling are given in Table 3 and Table 4, respectively. The normal refueling operation exchanges spent fuel assemblies after 1-year cooling, so the process removing at the peak burnup is not anticipated when the plant is running as scheduled.

In the second column of Table 3, the case that the removed fuel assembly at its peak burnup is placed in the lower position in cask is considered. The dose rate at the tally location 5 is the maximum as 3196.23 mrem/h, which is extremely high compared with the dose limit regulations [23–25]. The high radiation level at the tally 5 compared with other tallies is mainly due to a 100 mm penetration for the cooling air exit route around 5. The tally location 3 is the cask surface in the radial shielding direction. The dose rate at this location (with the maximum shielding) is 173.89 mrem/h, and this level is still unacceptable. Thus, it can be concluded that the energy level is too high for the fuel at its peak burn to be handled out of the vessel. In other words, the fuel needs to be cooled without considering removing the fuel at its peak, and the shielding thickness increase may not accommodate its design for the economic reason.

The third column of Table 3 gives the comparison of results between the fuel placement location in the cask. In the table, the dose rates were for the case with the same conditions with the results in the second column except for the fuel which is placed at a higher position in the cask. It is worth noting that the shielding results are about the same for the tally 3 in this case. The radial dose remains about the same for the FA's longitudinal movements, because a long rod-type FA is in a cylindrical shield, and the distance between FA surface and radial tallies does not vary for the axial motions of the FA. But, tallies 1 and 2 yielded increased dose rates while dose rates at tallies 4,5, and 6 far decreased. Particularly, the rate has been cut by 1/1000th at tally 3 from about 3000 mrem/h. Because the top and bottom of the cask shield are in the symmetry structure to the center of the cask, a high rate at tally 2 can be

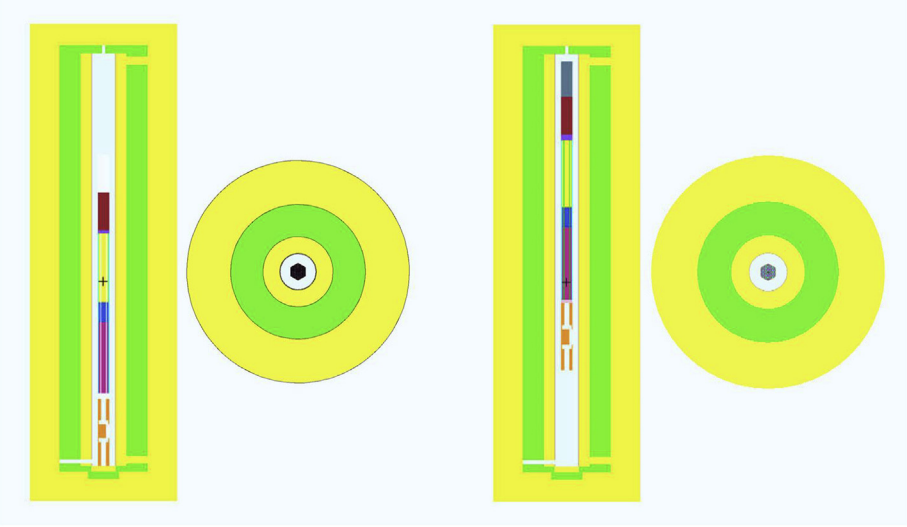

Fig. 9. MCNP6 model for evaluations of radiation dose.

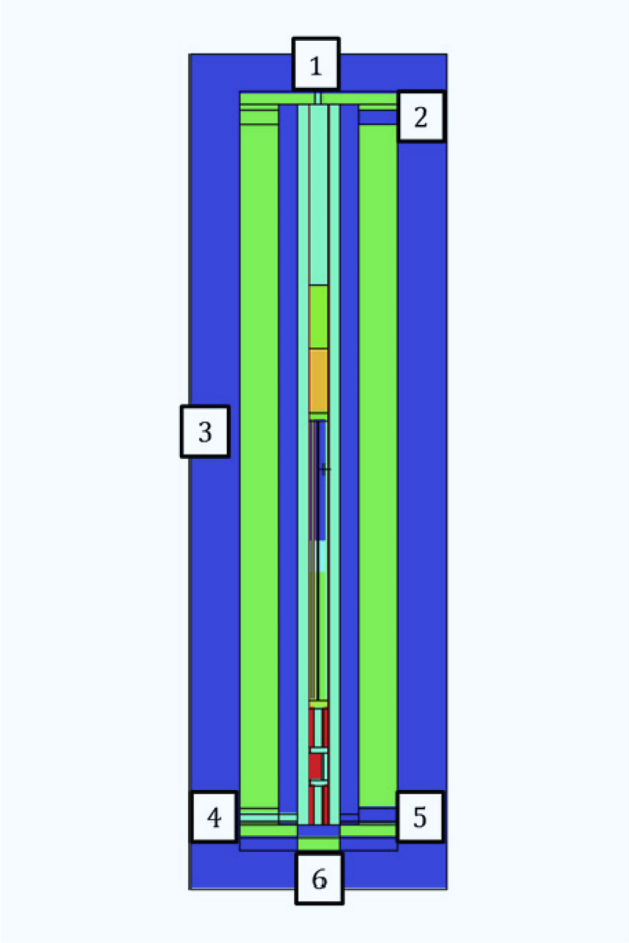

Fig. 10. MCNP6 tally location for the radiation dose.

Table 3
Photon dose rate by MCNP6 when FA removed at the peak burnup.

Tally location	FA at the bottom [mrem/hr]	FA at the top [mrem/hr]
1	71.75 ± 1.14	262.01 ± 2.75
2	18.82 ± 1.85	117.28 ± 8.22
3	173.89 ± 0.52	173.89 ± 0.052
4	114.59 ± 11.12	2.52 ± 0.547
5	3196.23 ± 137.44	33.59 ± 3.47
6	429.93 ± 0.86	23.95 ± 0.043

Table 4
Photon dose rate by MCNP6 when FA removed after 1-year cooling.

Tally location	FA at the bottom [mrem/hr]	FA at the top [mrem/hr]
1	4.96E-02 ± 1.34E-02	1.83E-01 ± 3.12E-02
2	6.10E-02 ± 1.34E-02	9.02E-01 ± 4.97E-01
3	7.80E-02 ± 3.12E-05	7.80E-02 ± 2.65E-04
4	2.06E-01 ± 6.36E-02	4.97E-03 ± 2.04E-03
5	11.34 ± 1.1261	4.83E-01 ± 1.56E-01
6	1.57E-01 ± 5.09E-03	1.00E-02 ± 2.78E-04

expected when the fuel is lifted high. But, it is interesting to see that the rate at tally 2 when the spent fuel assembly is located at the top is not as high as the one at tally 5 when the spent fuel assembly is located at the bottom. This is because the active fuel region is located lower than the center in the assembly to the bottom. For any positions of the spent fuel assembly inside the cask, the rates are high and not acceptable. The fuel needs to be cooled down in the vessel (or ex-vessel) confirmed by the results.

Table 4 shows the dose rates for the fuel remove after 1-year cooling, which is the normal refueling process. The rate has been cut by 1/2000th from ~173 mrem/h into ~0.08 mrem/h. The maximum rate is a relatively low level of 11.34 mrem/h for the tally 5 when the spent fuel is loaded low in the cask. For the spent fuel placed high, all dose rates are less than 2 mrem/h and are considered acceptable in terms of safety.

7. Conclusions

Sodium Fast Reactors (SFRs) require a distinct ex-vessel handling system unlike conventional Pressurized Water Reactors, including a fuel transfer cask, due to the unique working environment of SFRs. For the efficient design approach, Particle Swarm Optimization (PSO) was taken into account to set the initial design parameter of shielding thickness. Using the PSO algorithm, the values were converged as optimal after tens of iterations, which were inevitable for PSO. In the PSO process, a simplified model reflecting given design parameters was used for low calculation burden of iterations. The PSO process was quickly done in only a few iteration steps. Other PSO settings did not change the optimization result so much. Thus, for a U-10Zr spent fuel after 1-year cooling of the prototype reactor, the initial values were set as 290 mm and 150 mm for shielding and cooling.

Based on the initial setting, the full 3D cask model was constructed and evaluated for its shielding performance. For a normal refueling mode, with spent fuels removed after 1-year cooling period, the dose rates were acceptable in terms of safety except the air inlet tally location when the fuel is loaded at the lower position. If fuels are removed at its peak burnup, the radiation levels were very high and unable to be shielded with a typical cask dimension. Thus, the fuel needs to be cooled no matter what the reactor circumstances are, and the fuels should be lifted high in the cask.

Shielding performance was evaluated by calculating dose rates for two loading scenarios. Based on the configuration, a complete thermal-fluid (CFD) analysis remains for future work. The work will evaluate the heat removal capacity from a spent fuel assembly, which is another important design factor to be confirmed for its functional requirement.

Conflicts of interest

All authors have no conflicts of interest to declare.

Acknowledgments

This work was supported by a National Research Foundation of Korea (NRF) grant funded by the Korean government (Ministry of Science, ICT, and Future Planning) (No. NRF-2012M2A8A2025624).

Appendix A. Supplementary data

Supplementary data to this article can be found online at https://doi.org/10.1016/j.net.2018.09.007.

References

[1] T. Abram, S. Ion, Generation-IV nuclear power: a review of the state of the science, Energy Pol. 36 (12) (2008) 4323–4330.
[2] J. Rouault, et al., Sodium fast reactor design: fuels, neutronics, thermal-hydraulics, structural mechanics and safety, in: Handbook of Nuclear Engineering, Springer, 2010, pp. 2321–2710.
[3] Y. Chikazawa, M. Farmer, C. Grandy, Technology gap analysis on sodium-cooled reactor fuel-handling system supporting advanced burner reactor

development, Nucl. Technol. 165 (3) (2009) 270–292.
[4] R.T. Klann, B.A. Picker Jr., A conceptual redesign of an inter-building fuel transfer cask, in: Proceedings of 2nd ASME-JSME International Conference on Nuclear Engineering, San Francisco, CA, USA, March 21-24, 1993.
[5] B.C. Cerutti, et al., EBR-II fuel handling system, in: Proceedings of Symposium on Progress in Sodium-cooled Fast Reactor Engineering, Monaco, March 23-27, 1970.
[6] D. Madden, E. Garrett, Design of the FFTF fuel handling systems bottom loading transfer casks, in: Tech. rep., Aerojet Mfg. Co., Fullerton, Calif.(USA), Westinghouse Hanford Co., Richland, Wash.(USA), 1973.
[7] P. Puthiyavinayagam, et al., Development of fast breeder reactor technology in India, Prog. Nucl. Energy 101 (2017) 19–42.
[8] B. Sodhi, et al., Conceptual Design of Core Component Handling System in PFBR, 1996. IAEA-TECDOC-907.
[9] F. Dechelette, et al., Study and Evaluation of Innovative Fuel Handling Systems for Sodium-cooled Fast Reactors: Fuel Handling Route Optimization, Science and Technology of Nuclear Installations, 2014. Article ID 254913.
[10] N. Kawasaki, et al., Design study for reactor system of fast reactor JSFR-concept of reactor system, in: Proceedings of the ICAPP2015, Nice, France, May 3-6, 2015.
[11] Y. Chikazawa, et al., JSFR key technology evaluation on fuel handling system, J. Nucl. Sci. Technol. 51 (4) (2014) 437–447.
[12] J. Yoo, et al., Overall system description and safety characteristics of prototype gen-IV sodium cooled fast reactor in Korea, Nuclear Engineering and Technology 48 (5) (2016) 1059–1070.
[13] R. Eberhart, J. Kennedy, A new optimizer using particle swarm theory, in: Proceedings of the Sixth International Symposium on Micro Machine and Human Science, Nagoya, Japan, October 4-6, 1995.
[14] J. Kennedy, Particle swarm optimization, in: Encyclopedia of Machine Learning, Springer, 2011, pp. 760–766.
[15] R. l. Perez, K. Behdinan, Particle swarm approach for structural design optimization, Comput. Struct. 85 (19–20) (2007) 1579–1588.
[16] X. Hu, R.C. Eberhart, Y. Shi, Engineering optimization with particle swarm, in: Proceedings of the 2003 IEEE Swarm Intelligence Symposium, Indianapolis, IN, USA, April 26, 2003.
[17] R. Hassan, et al., A comparison of particle swarm optimization and the genetic algorithm, in: 46th AIAA/ASME/ASCE/AHS/ASC Structures, Structural 590 Dynamics and Materials Conference, 2005, p. 1897.
[18] D. Pelowitz (Ed.), MCNP6 User's Manual Version 1.0, LA-CP-13-00634, Los Alamos National Laboratory, 2013.
[19] J.H. Ko, et al., Shielding analysis of dual purpose casks for spent nuclear fuel under normal storage conditions, Nuclear Engineering and Technology 46 (4) (2014) 547–556.
[20] M. Asami, K. Sawada, A. Konnai, N. Odano, Application of dose evaluation of the MCNP code for the spent fuel transport cask, Progress of Nuclear Science and Technology 2 (2011) 855–859.
[21] IAEA, Regulations for the Safe Transport of Radioactive Material, International Atomic Energy Agency, 2012. IAEA Safety Standards No. SSR-6.
[22] A.G. Croff, User's Manual for the ORIGEN2 Computer Code, ORNL/TM-7175, Oak Ridge National Laboratory, 1980.
[23] US Nuclear Regulatory Commission, NRC Regulations Title 10, Code of Federal Regulations (10 CFR), Part 20-standards for protection against radiation, https://www.nrc.gov/reading-rm/doc-collections/cfr/part020/, page accessed Friday, February 16, 2018.
[24] US Nuclear Regulatory Commission, Standard Review Plan for Spent Fuel Dry Storage Facilities: Final Report, 2000. NUREG-1567.
[25] Nuclear Safety & Security Commission, Standards for Safe Operation of Radioactive Materials, http://www.law.go.kr, page accessed on Friday, June 1st, 2018.